

# The Extended Baryonic Halo of NGC 3923

Bryan W. Miller<sup>1,\*</sup> , Tomás Ahumada<sup>1</sup>, Thomas H. Puzia<sup>2</sup>, Graeme N. Candlish<sup>3</sup>, Stacy S. McGaugh<sup>4</sup> , J. Christopher Mihos<sup>4</sup>, Robyn E. Sanderson<sup>5</sup>, Mischa Schirmer<sup>1</sup> , Rory Smith<sup>6</sup> and Matthew A. Taylor<sup>7</sup>

<sup>1</sup> Gemini Observatory, Casilla 603, La Serena 1700000, Chile; tahumada@gemini.edu (T.A.); mschirmer@gemini.edu (M.S.)

<sup>2</sup> Institute of Astrophysics, Pontificia Universidad Católica de Chile, Santiago 7820436, Chile; tpuzia@astro.puc.cl

<sup>3</sup> Physics and Astronomy Institute, Universidad de Valparaíso, Valparaíso 2360102, Chile; graeme.candlish@ifa.uv.cl

<sup>4</sup> Department of Astronomy, Case Western Reserve University, Cleveland, OH 44106, USA; stacy.mcgaugh@case.edu (S.S.M.); mihos@case.edu (J.C.M.)

<sup>5</sup> Department of Astronomy, California Institute of Technology, Pasadena, CA 91125, USA; robyn.sanderson@gmail.com

<sup>6</sup> Optical Astronomy Division, Korea Astronomy and Space Science Institute, Daedeokdae-ro 776, Yuseong-gu, Daejeon 34055, Korea; rorysmith274@gmail.com

<sup>7</sup> Gemini Observatory, Hilo, HI 96720, USA; mtaylor@gemini.edu

\* Correspondence: bmiller@gemini.edu; Tel.: +56-51-2205618

Academic Editors: Emilio Elizalde, Duncan A. Forbes and Ericson D. Lopez

Received: 1 July 2017; Accepted: 14 July 2017; Published: 20 July 2017

**Abstract:** Galaxy halos and their globular cluster systems build up over time by the accretion of small satellites. We can learn about this process in detail by observing systems with ongoing accretion events and comparing the data with simulations. Elliptical shell galaxies are systems that are thought to be due to ongoing or recent minor mergers. We present preliminary results of an investigation of the baryonic halo—light profile, globular clusters, and shells/streams—of the shell galaxy NGC 3923 from deep Dark Energy Camera (DECam) *g* and *i*-band imaging. We present the 2D and radial distributions of the globular cluster candidates out to a projected radius of about 185 kpc, or  $\sim 37R_e$ , making this one of the most extended cluster systems studied. The total number of clusters implies a halo mass of  $M_h \sim 3 \times 10^{13} M_\odot$ . Previous studies had identified between 22 and 42 shells, making NGC 3923 the system with the largest number of shells. We identify 23 strong shells and 11 that are uncertain. Future work will measure the halo mass and mass profile from the radial distributions of the shell, N-body models, and line-of-sight velocity distribution (LOSVD) measurements of the shells using the Multi Unit Spectroscopic Explorer (MUSE).

**Keywords:** galaxies: elliptical and lenticular, cD; galaxies: halos; galaxies: individual (NGC 3923); galaxies: structure; galaxies: star clusters: general

## 1. Introduction

Galaxies at high redshift are much more compact at a given mass than in the local universe, implying that galaxies and their halos grow with time due to the accretion of mostly lower-mass galaxies [1–3]. Therefore, we can learn about the details of this process by observing nearby systems that are in the process of merging or accreting. Merger remnants and galaxies with tidal streams are good candidates. Elliptical shell galaxies are other promising environments for studying the build-up of halos. Shell galaxies are surrounded by interleaved “umbrellas” or shells of stellar material that

match the appearance of structures created during the accretion of low-mass satellites on near-radial orbits in simulations (Figure 1) [4].

In this contribution, we present preliminary results of a study of the globular cluster system and shells of the elliptical shell galaxy NGC 3923. NGC 3923 is one of the most studied shell galaxies because it has the largest number of detected shells. Different studies have identified between 22 and 42 shells [5,6]. Therefore, new, deeper data will help determine the true number of shells and look for additional shells at larger radii. Mergers will also bring in new globular clusters (GCs) so the distribution and total number of GCs can be used to estimate the halo mass. We adopt a distance to NGC 3923 of  $21.3 \pm 1.4$  Mpc ( $(m - M)_0 = 31.64 \pm 0.14$ ) [7]. Using a total apparent magnitude of  $V_T^0 = 9.69$  [8] results in an absolute magnitude of  $M_V = -21.95$ .

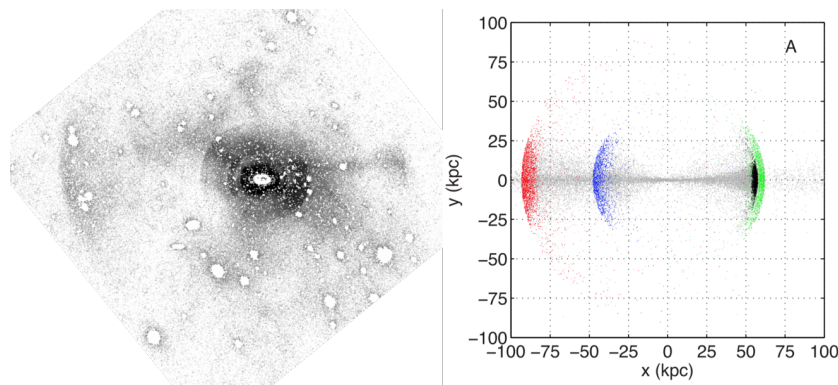


**Figure 1.** The observed shells around NGC 3923 (left panel) compared with the distribution of particles stripped from an accreting satellite galaxy on a radial orbit in an N-body simulation (right panel; reproduced from Figure 3 of [4]). The underlying light of the galaxy has been removed from the image using the ARCHANGEL ellipse-fitting package [9]. The simulation is of a  $2.2 \times 10^8 M_\odot$  satellite falling into a spherical potential with total mass of  $2.7 \times 10^{12} M_\odot$ .

## 2. Observations and Reduction

NGC 3923 was observed on 22–23 April 2015 using Dark Energy Camera (DECam) on the Blanco 4-m telescope at the Cerro Tololo Inter-American Observatory (CTIO) [10]. The conditions were photometric with seeing of about 1 arcsec. Total integration times of 10,400 sec in  $g'$ -band and 10,800 sec in  $i'$ -band were obtained. A Fermat spiral dither pattern was used to maximize uniformity across the gaps between the 62 detectors. Sky subtraction is critical since we are searching for low-surface brightness features on scales of a degree on the sky. Therefore, exposures alternated between the NGC 3923 field and five different sky fields (Figure 2).

These observations were done as part of the larger *Neighborhood Watch* survey of the baryonic structures within about 20 Mpc using DECam  $u'g'i'$  and VIRCAM  $J$  and  $K_s$  imaging. The goals are to use globular clusters, dwarf galaxies, and shells to study stellar populations and the formation of structures in the local universe. Targets include the Fornax Cluster and the CenA, Sombrero, NGC 2997, NGC 6744, and NGC 3115 groups.

The sky-subtraction algorithms used by the DECam community pipeline [11] are not designed for extended objects and over-subtract the sky in the vicinity of large, bright galaxies. Therefore, we reduced the data using the THELI reduction software [12] that used the images of the sky fields to create the background model. This eliminated the problem of sky over-subtraction.

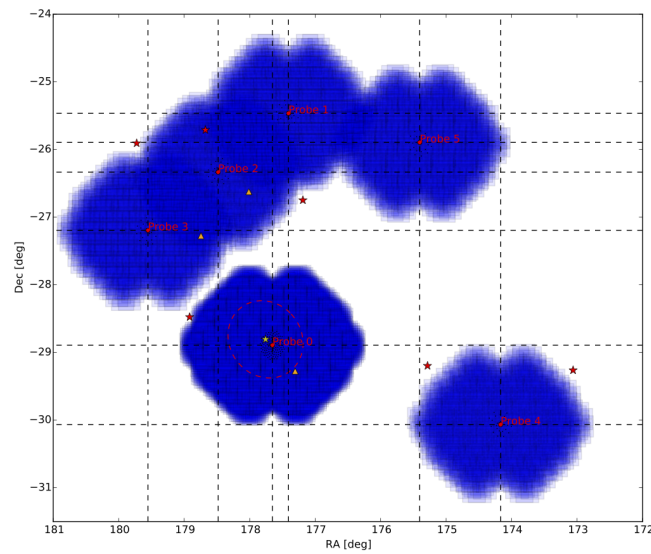


**Figure 2.** DECam observing strategy for NGC 3923. The yellow star marks the center of NGC 3923 and the red dashed circle indicates the approximate extent of the shell system. Red stars indicate bright foreground stars that we attempted to avoid. Orange diamonds indicate other objects of interest. The sky fields (Probes 1–5) were selected to not have bright galaxies or extended structures.

### 3. Results

#### 3.1. The Globular Cluster System

At a distance of 21.3 Mpc, GCs are unresolved from the ground in 1 arcsec seeing. Therefore, we identified candidate GCs by selecting objects consistent with being point sources and then doing statistical background subtraction. The candidate GCs from [13]—taken in much better image quality using GMOS-S—were used as a “training” set to guide our selection. Source detection and photometry were done using SExtractor and PSFEx [14,15]. Principal component analysis (PCA) was applied to the photometry parameters in order to select point sources (Figure 3a). The eigenvectors are dominated by the FLUX\_RADIUS and SPREAD\_MODEL parameters. We then applied cuts in color-magnitude space as shown in Figure 3b. Finally, we fit a plane to the source density of objects more than 30 arcmin from NGC 3923, and statistically (randomly) subtracted this background.

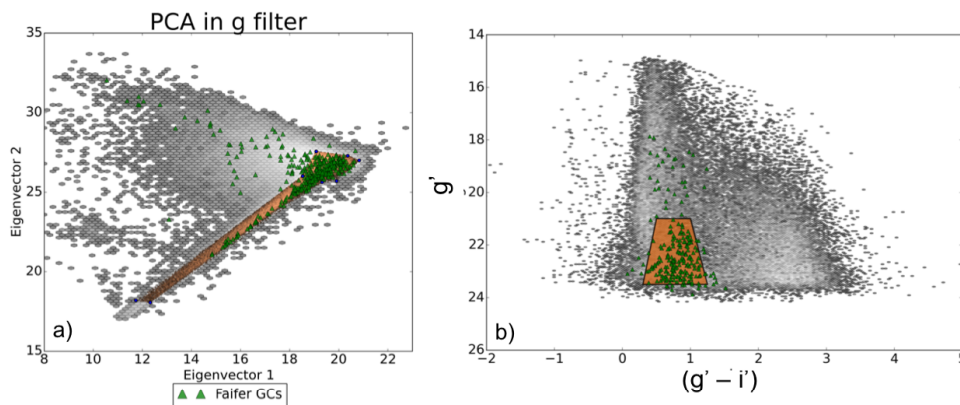


**Figure 3.** (a) Star+globular cluster (GC)/galaxy separation using principal component analysis (PCA). Most of the power is in the FLUX\_RADIUS and SPREAD\_MODEL parameters. Green triangles represent GCs and ultra-compact dwarfs (UCDs) from [13]. (b) Globular cluster candidates were then selected to be in the orange polygon in the color-magnitude diagram (CMD).

This process resulted in the selection of 500 candidate GCs detected by DECam within a projected radius of 0.5 degree, which corresponds to 185 kpc, about  $37R_e$  (Figure 4a). This makes the NGC 3923 globular cluster system (GCS) one of the most extended known, comparable to the GCSs of the Milky Way and M31 [16]. This is mainly due to the very wide-field imaging used here. As other galaxies are observed on this scale, we expect that most GCSs of massive galaxies will be found to have similar extents.

In the GCSs of other elliptical galaxies, the “blue” and “red” GCs usually have different radial distributions [13]. We explore the radial distributions of the NGC 3923 GCs by dividing the candidates at  $(g' - i') = 0.85$ , the minimum between the blue and red color peaks from [13], and plotting the radial distributions in Figure 4b. For this and further analysis, we include 249 GCs from [13] that are detected closer to the center of the galaxy than our current method can find. As found in previous work, the distribution of the blue GCs is more extended than that of the red GCs. The colors of the blue GCs are consistent with the colors of GCs in dwarf galaxies [17,18], and spectroscopic abundances show that the blue clusters are more metal-poor than the red clusters [19]. This is evidence that the two populations are distinct and may have had different formation histories. It is commonly thought that many of the blue GCs may have been accreted from merging dwarf galaxies, but the orbits of outer GCs can be unexpectedly tangential (see [19]), so more kinematic information is needed to test this hypothesis.

The total number of GCs associated with NGC 3923 can be estimated by integrating over the globular cluster luminosity function (GCLF). Following [20], we assume that the GCLF is a Gaussian with a peak at  $M_g^0 = -7.2$  or  $g^0 = 24.44$ . Completeness tests have not been performed yet, so the faint magnitude limit ( $g' = 23.5$ ) was chosen to be well below the magnitude where incompleteness is significant. Fitting the observed luminosity function gives a reasonable Gaussian sigma of 1.4 mag and 3142 total clusters. This gives a globular cluster specific frequency of  $S_N = N_{GC}10^{0.4(M_V+15)} = 5.2$ , similar to previous results [13].

Harris et al. (2017) [21] has shown that the total number of GCs is proportional to the total halo mass. With this method, the 3142 GCs in NGC 3921 imply a halo mass of  $M_h \sim 3.5 \times 10^{13} M_\odot$ . This compares to a dynamical mass of  $M_{dyn} \sim 2 \times 10^{12} M_\odot$  at 30 kpc [22].

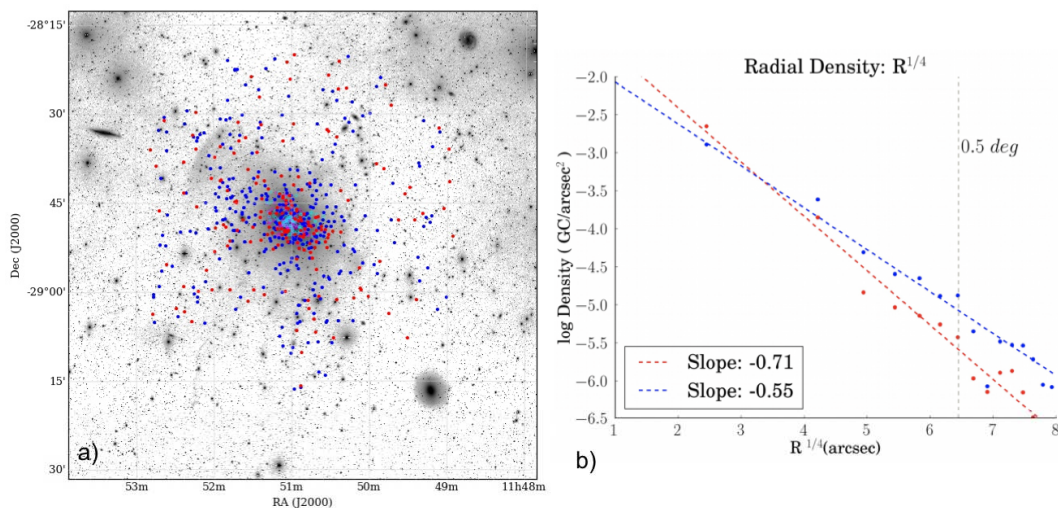


**Figure 4.** (a) Dark Energy Camera (DECam)  $g'$ -band image with GC candidates indicated. Magenta and cyan points are GC candidates from [13], while the red and blue points are DECam detections. Magenta and red points indicate the “red” objects with  $(g' - i') \geq 0.85$ , while cyan and blue points are for “blue” objects with  $(g' - i') < 0.85$ . (b) The radial distributions of the “red” and “blue” GC candidates as separated in panel a). As in other galaxies, the bluer GC candidates have a more extended distribution.

### 3.2. Shells

The shells around NGC 3923 were identified by eye after removing the underlying galaxy light. The galaxy subtraction was done using a two-Sersic model with *Imfit* image-fitting code [23]. We also enhanced the shell edges in the inner regions by applying an erosion filter edge detection algorithm [5]. The results are given in Figure 5. We have identified 23 strong shells in common with [5]. Eleven shells are classified as uncertain, and eight shells from [5] are not detected. No new shells have been detected yet, but analysis is ongoing.

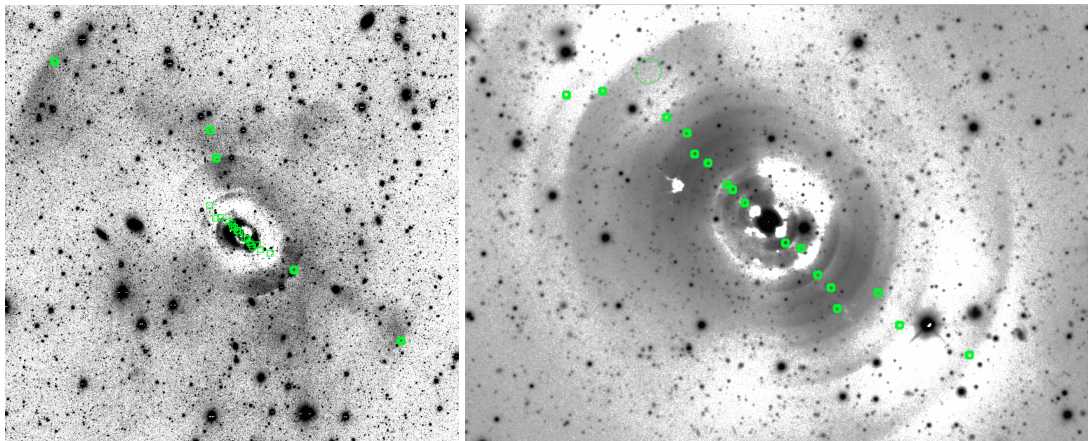


**Figure 5.** The green squares mark the rims of the clear, strong shells identified in NGC 3923. The underlying background galaxy light has been removed by fitting a two-Sersic model with *Imfit* [23]. The left panel shows the full shell system and the right panel is an expanded view of the inner region.

The shells from a single minor merger should have an alternating, or interleaved, pattern relative to the center of the galaxy. The pattern for the 23 strong shells that we identified in NGC 3923 is shown in Figure 6. The pattern does not alternate as expected. In future work we will look for multiple patterns and additional shells. The spacing of the shells can then be used to constrain the potential and the enclosed mass [24].

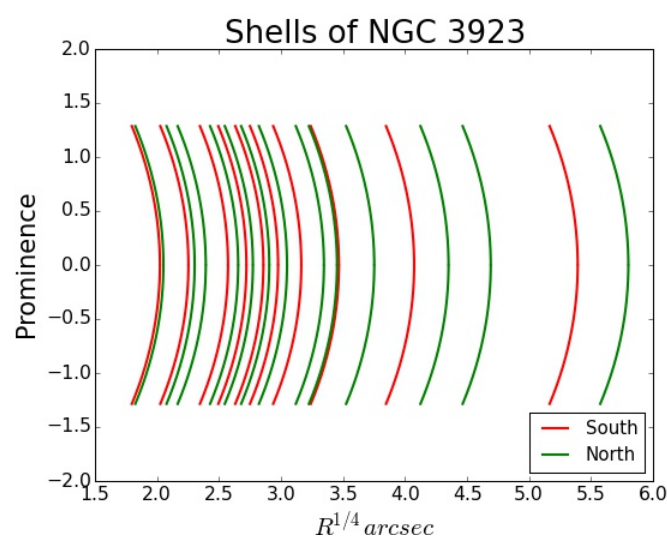


**Figure 6.** A representation of the interleaving pattern of the shells in NGC 3923.  $R$  is the projected radius of the shell rim from the galaxy center. Green arcs indicate shells to the north of the center and red arcs are those to the south. Red and green arcs should alternate, but the outer shells do not follow this pattern.

#### 4. Summary and Future Work

In this work we have identified and characterized the GCs and shells in the halo of NGC 3923. A total of 500 GC candidates are detected in deep DECam imaging out to a projected radius of 185 kpc. This implies a total GC population of about 3100 and a halo mass of  $\mathcal{M}_h \sim 3 \times 10^{13} M_\odot$ . In continuing work, we are trying to detect fainter sources and characterize the photometric completeness. Twenty-three interleaved shells are confirmed, and so far we have not detected previously uncatalogued shells. We are currently applying edge-detection and other algorithms that may be useful for detecting, defining, and characterizing the shells.

Future analysis will focus on deriving the mass profile of NGC 3923 out to a projected radius of about 130 kpc. We will use N-body simulations to reproduce the positions and morphologies of the shells and the velocities of satellite galaxies. This will put constraints on the shape and profile of the potential. Measuring the kinematics of the GCs will also be extremely important. Finally, we will be using the Multi Unit Spectroscopic Explorer (MUSE) instrument on the European Southern Observatory Very Large Telescope (ESO VLT) to measure the line-of-sight velocity distribution (LOSVD) of the stars in the low-surface brightness shells themselves ( $B \sim 27$  mag arcsec<sup>2</sup>). Fitting the width of the LOSVD with radius from the shell edge can give the gravitational acceleration and the enclosed mass at the shell edge [4].

Elliptical shell galaxies are excellent systems for studying the extent of galaxy halos and the processes that form them. They allow us to use the multiple constraints of globular clusters, shells, and satellite companions to constrain models of their structure and formation.

**Acknowledgments:** Based on observations at Cerro Tololo Inter-American Observatory, National Optical Astronomy Observatory (NOAO Prop. ID: 2015A-0630; PI: T. Puzia), which is operated by the Association of Universities for Research in Astronomy (AURA) under a cooperative agreement with the National Science Foundation. Funding for the DES Projects has been provided by the DOE and NSF (USA), MISE (Spain), STFC (UK), HEFCE (UK), NCSA (UIUC), KICP (U. Chicago), CCAPP (Ohio State), MIFPA (Texas A&M), CNPQ, FAPERJ, FINEP (Brazil), MINECO (Spain), DFG (Germany) and the collaborating institutions in the Dark Energy Survey, which are Argonne Lab, UC Santa Cruz, University of Cambridge, CIEMAT-Madrid, University of Chicago, University College London, DES-Brazil Consortium, University of Edinburgh, ETH Zürich, Fermilab, University of Illinois, ICE (IEEC-CSIC), IFAE Barcelona, Lawrence Berkeley Lab, LMU München and the associated Excellence Cluster Universe, University of Michigan, NOAO, University of Nottingham, Ohio State University, University of Pennsylvania, University of Portsmouth, SLAC National Lab, Stanford University, University of Sussex, and Texas A&M University. This research has made use of the NASA/IPAC Extragalactic Database (NED) which is operated by the Jet Propulsion Laboratory, California Institute of Technology, under contract with the National Aeronautics and Space Administration. This research made use of Astropy, a community-developed core Python package for Astronomy [25].

**Author Contributions:** B.W.M. and T.H.P. conceived and designed the experiment. B.W.M. wrote this paper. T.A. reduced the data and performed the detection and photometry of the GCs and shells. S.S.M., J.C.M., M.A.T., and M.S. assisted with the observing strategy, data reduction, and analysis. R.E.S., G.N.C., and R.S. provided simulations and theoretical analysis of the shells.

**Conflicts of Interest:** The authors declare no conflict of interest.

#### Abbreviations

The following abbreviations are used in this manuscript:

CMD	Color-Magnitude Diagram
CTIO	Cerro Tololo Inter-American Observatory
DECam	Dark Energy Camera
ESO	European Southern Observatory
GC	Globular Cluster
GCLF	Globular Cluster Luminosity Function
GCS	Globular Cluster System

GMOS-S	Gemini Multi-Object Spectrograph - South
LOSVD	Line-of-Sight Velocity Distribution
MUSE	Multi Unit Spectroscopic Explorer
PCA	Principal Component Analysis
UCD	Ultra-Compact Dwarf
VLT	Very Large Telescope

## References

1. Carrasco, E.R.; Conselice, C.J.; Trujillo, I. Gemini K-band NIRI Adaptive Optics Observations of massive galaxies at  $1 < z < 2$ . *Mon. Not. Roy. Astro. Soc.* **2010**, *405*, 2253.
2. Oser, L.; Ostriker, J.P.; Naab, T.; Johansson, P.H.; Burkert, A. The Two Phases of Galaxy Formation. *Astrophys. J.* **2010**, *725*, 2312.
3. Van Dokkum, P.G.; Nelson, E.J.; Franx, M.; Oesch, P.; Momcheva, I.; Brammer, G.; Schreiber, N.M.F.; Skelton, R.E.; Whitaker, K.E.; van der Wel, A.; et al. Forming Compact Massive Galaxies. *Astrophys. J.* **2015**, *813*, 23.
4. Sanderson, R.E.; Helmi, A. An analytical phase-space model for tidal caustics. *Mon. Not. Roy. Astro. Soc.* **2013**, *435*, 378.
5. Bílek, M.; Cuillandre, J.C.; Gwyn, S.; Ebrova, I.; Bartořkova, K.; Jungwiert, B.; Jilkova, L. Deep imaging of the shell elliptical galaxy NGC 3923 with MegaCam. *Astron. Astrophys.* **2016**, *588*, A77.
6. Prieur, J.L. The shell system around NGC 3923 and its implications for the potential of the galaxy. *Astrophys. J.* **1988**, *326*, 596.
7. Tully, R.B.; Courtois, H.M.; Dolphin, A.E.; Fisher, J.R.; Heraudeau, P.; Jacobs, B.A.; Karachentsev, I.D.; Makarov, D.; Makarova, L.; Mitronova, S.; et al. Cosmicflows-2: The Data. *Astron. J.* **2013**, *146*, 86.
8. De Vaucouleurs, G.; de Vaucouleurs, A.; Corwin, H.G., Jr.; Buta, R.J.; Paturel, G.; Fouque, P. *Third Reference Catalog of Bright Galaxies (RC3)*; Springer: New York, NY, USA, 1991.
9. Schombert, J. ARCHANGEL Galaxy Photometry System. *arXiv* **2007**, arXiv:astro-ph/0703646.
10. Flaugher, B.; Diehl, H.T.; Honscheid, K.; Abbott, T.M.C.; Alvarez, O.; Angstadt, R.; Annis, J.T.; Antonik, M.; Ballester, O.; Beaufore, L.; et al. The Dark Energy Camera. *Astron. J.* **2015**, *150*, 43.
11. Valdes, F.; Gruendl, R. DES Project The DECam Community Pipeline. *ASP Conf. Ser.* **2014**, *485*, 379.
12. Schirmer, M. THELI: Convenient Reduction of Optical, Near-infrared, and Mid-infrared Imaging Data. *Astrophys. J. Suppl.* **2013**, *209*, 21.
13. Faifer, F.R.; Forte, J.C.; Norris, M.A.; Bridges, T.; Forbes, D.A.; Zepf, S.E.; Beasley, M.; Gebhardt, K.; Hanes, D.A.; Sharples, R.M. Gemini/GMOS imaging of globular cluster systems in five early-type galaxies. *Mon. Not. Roy. Astro. Soc.* **2011**, *416*, 155.
14. Bertin, E. Automated Morphometry with SExtractor and PSFEx. *ASP Conf. Ser.* **2011**, *442*, 435–438.
15. Bertin, E.; Arnouts, S. SExtractor: Software for source extraction. *Astron. Astrophys. Suppl.* **1996**, *117*, 393.
16. Huxor, A.P.; Mackey, A.D.; Ferguson, A.M.N.; Irwin, M.J.; Martin, N.F.; Tanvir, N.R.; Veljanoski, J.; McConnachie, A.; Fishlock, C.K.; Ibata, R.; et al. The outer halo globular cluster system of M31 - I. The final PAndAS catalogue. *Mon. Not. Roy. Astro. Soc.* **2014**, *442*, 2165–2187.
17. Lotz, J.M.; Miller, B.W.; Ferguson, H.C. The Colors of Dwarf Elliptical Galaxy Globular Cluster Systems, Nuclei, and Stellar Halos. *Astrophys. J.* **2004**, *613*, 262.
18. Peng, E.W.; Jordan, A.; Cote, P.; Blakeslee, J.P.; Ferrarese, L.; Mei, S.; West, M.J.; Merritt, D.; Milosavljevic, M.; Tonry, J.L. The ACS Virgo Cluster Survey. IX. The Color Distributions of Globular Cluster Systems in Early-Type Galaxies. *Astrophys. J.* **2006**, *639*, 95.
19. Brodie, J.B.; Romanowsky, A.J.; Strader, J.; Forbes, D.A.; Foster, C.; Jennings, Z.G.; Pastorello, N.; Pota, V.; Ushe, C.; Blom, C.; et al. The SAGES Legacy Unifying Globulars and GalaxieS Survey (SLUGGS): Sample Definition, Methods, and Initial Results. *Astrophys. J.* **2014**, *796*, 52.
20. Jordan, A.; McLaughlin, D.; Cote, P. The ACS Virgo Cluster Survey. XII. The Luminosity Function of Globular Clusters in Early-Type Galaxies. *Astrophys. J. Suppl.* **2007**, *171*, 101–145.
21. Harris, W.E.; Blakeslee, J.P.; Harris, G.L.H. Galactic Dark Matter Halos and Globular Cluster Populations. III. Extension to Extreme Environments. *Astrophys. J.* **2017**, *836*, 67.

22. Norris, M.A.; Gebhardt, K.; Sharples, R.M.; Faifer, F.R.; Bridges, T.; Forbes, D.A.; Forte, J.C.; Zepf, S.E.; Beasley, M.A.; Hanes, D.A.; et al. The globular cluster kinematics and galaxy dark matter content of NGC 3923. *Mon. Not. Roy. Astro. Soc.* **2012**, *421*, 1485–1498.
23. Erwin, P. Imfit: A Fast, Flexible New Program for Astronomical Image Fitting. *Astrophys. J.* **2015**, *799*, 226.
24. Hernquist, L.; Quinn, P.J. Shells and Dark Matter in Elliptical Galaxies. *Astrophys. J.* **1987**, *312*, 1.
25. Astropy Collaboration; Robitaille, T.P.; Tollerud, E.J.; Greenfield, P.; Droettboom, M.; Bray, E.; Aldcroft, T.; Davis, M.; Ginsburg, A.; Price-Whelan, A.M.; et al. Astropy: A community Python package for astronomy. *Astron. Astrophys.* **2013**, *558*, A33.



© 2017 by the authors. Licensee MDPI, Basel, Switzerland. This article is an open access article distributed under the terms and conditions of the Creative Commons Attribution (CC BY) license (<http://creativecommons.org/licenses/by/4.0/>).